PHYSICAL REVIEW A **71**, 021401(R) (2005)

High-density mesoscopic atom clouds in a holographic atom trap

J. Sebby-Strabley, R. T. R. Newell,* J. O. Day, E. Brekke, and T. G. Walker
Department of Physics, University of Wisconsin—Madison, Madison, Wisconsin 53706, USA
(Received 11 November 2004; published 9 February 2005)

We demonstrate the production of micron-sized high-density atom clouds of interest for mesoscopic quantum information processing. We evaporate atoms from 60 μK, 3×10^{14} atoms/cm^3 samples contained in a highly anisotropic optical lattice formed by interfering diffracted beams from a holographic phase plate. After evaporating to 1 μK by lowering the confining potential, in less than a second the atom density reduces to 8×10^{13} cm^{-3} at a phase space density approaching unity. Adiabatic recompression of the atoms then increases the density to levels in excess of 1×10^{15} cm^{-3}. The resulting clouds are typically 8 μm in the longest dimension. Such samples are small enough to enable mesoscopic quantum manipulation using the Rydberg blockade and have the high densities required to investigate collision phenomena.

DOI: 10.1103/PhysRevA.71.021401 PACS number(s): 32.80.Pj, 39.25.+k, 39.10.+j

Two of the most important themes in current studies of ultracold incoherent matter are studies of plasmas and Rydberg atoms at low temperature and high density, and the use of mesoscopic samples for topics in quantum information processing. Even at the relatively modest 10^{12} cm^{-3} densities of standard magneto-optical traps, a wide variety of phenomena has been observed by exciting atoms near their ionization limits [1]. Similarly, the use of atomic ensembles with their collectively enhanced light-atom interactions have led to developments such as collective spin squeezing [2], quantum memory [3], and single-photon generation [4]. With these contexts in mind, in this paper we report techniques for producing high density ($>10^{15}$ cm^{-3}) mesoscopic (5–10 μm) samples ideal for use in both types of experiments.

In the context of high densities, we note that the recent predictions of ultra-long-range Rydberg molecular states [5–7] require extremely high densities to attain significant production rates. These "trilobite" molecules arise from the Fermi pointlike interactions between Rydberg and ground-state atoms. At the densities reported here, the Fermi shifts of the Rydberg levels are on the order of 100 MHz. Similarly, the production of cold plasmas and Rydberg gases at these densities promises to reveal phenomena not accessible in conventional laser traps, which have 100–1000 times lower densities.

Regarding mesoscopic atom samples, Lukin *et al.* [8] recently proposed manipulating quantum information using the very-long-range dipole-dipole interactions produced by Rydberg atoms. In brief, the excitation of a single Rydberg atom strongly suppresses the excitation of other atoms within its range of influence. If the size of a sample of atoms is less than the blockade range R, then the accessible quantum states of the ensemble are limited to states of zero or one atom excitations. Using Rydberg states as intermediate states in the Rabi manipulation of two hyperfine ground states then allows the production of stable but highly entangled collective excitations of the ensembles. For MHz-rate quantum manipulations with cw lasers, the value of R required is a few μm at the principal quantum numbers $n>50$ [9]. The clouds produced in this experiment reach this length scale.

Recent experiments have demonstrated dramatic suppression of pulsed Rydberg state excitation in magneto-optical traps of size $L\gg R$ [10,11]. In these experiments, the number of excited Rydberg atoms saturates at fluence values much less than expected for isolated atoms due to the Rydberg-Rydberg interactions shifting atoms out of resonance with the exciting lasers. If the Rydberg blockade is effective, the number of excited atoms should be limited to roughly $(L/R)^3$. If the blockade is not complete, saturation still occurs but with a greater number of excited atoms. Thus to differentiate blockade and suppression requires the production of mesoscopic samples of size $L\sim R$ [12].

In this paper we present a method for producing high-density elliptical mesoscopic atom samples with semimajor axes σ on the order of R using rapid evaporative cooling of ^{87}Rb atoms from a holographic atom trap (HAT), followed by adiabatic recompression. We demonstrate densities in excess of 10^{15} cm^{-3}, the highest cold-atom densities attained for incoherent matter and an order of magnitude larger than previously reported densities [13]. The recompression stage can produce clouds with radii as small as 5.6 μm, a factor of four improvement, and are now sufficiently small to be sensitive to a single-atom Rydberg blockade.

The HAT, described in detail elsewhere [13], is a lattice of interference fringes produced by imaging five diffracted orders (zeroth order plus four equal intensity first-order beams) from a holographic phase plate. The laser used is an 18 W cw flashlamp-pumped Nd:YAG (Yttrium aluminum garnet) laser at 1.064 μm, intensity stabilized and controlled using an acousto-optic modulator feedback system. Along the propagation axis the Talbot effect gives rise to a series of interference fringes. Each Talbot fringe contains a lattice with a unit cell of 10 μm$\times$10 μm$\times$100 μm as illustrated in Fig. 1. The five diffracted orders are focused to approximately 90 μm waists at the region of intersection, giving a typical full-intensity trap depth of $U_0=600$ μK, and trap oscillation frequencies of 18.4 ± 1.2 kHz, 18.4 ± 1.2 kHz, and 735 ± 62 kHz. Atoms are loaded into the HAT from a forced-dark-spot $F=1$ magneto-optical trap [14].

We use absorption imaging to characterize the spatial dis-

*Present address: Los Alamos National Laboratory, Los Alamos, NM 87545, USA.

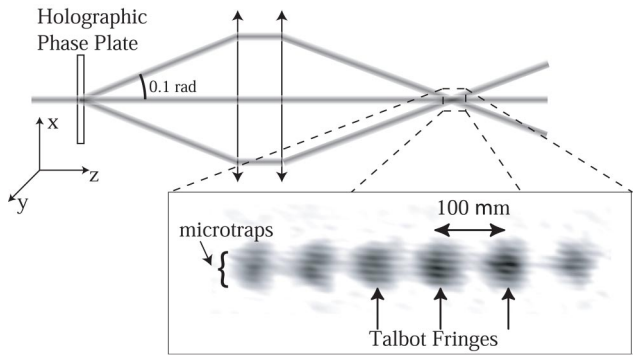

FIG. 1. Holographic atom trap: five laser beams (only three are visible from this perspective) diffracted from a phase plate are imaged onto a magneto-optical trap (MOT) cloud. Atoms collect in the intensity maxima of the interference pattern of the beams.

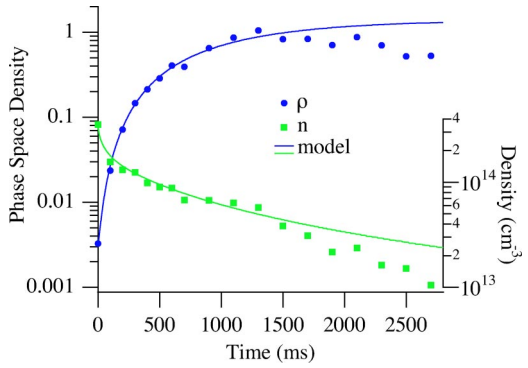

FIG. 2. During forced evaporation the phase space density ρ in the center microtrap approaches unity while the density n decreases with atom loss.

tribution of the atoms in the HAT, to make absolute measurements of the number of atoms, and to measure the atomic temperature via time-of-flight techniques. The HAT is first turned off in 10μs in order to eliminate ac Stark shifts and excited state hyperfine mixing. Then a 150-μs pulse of light from a diode laser tuned to the $5S_{1/2}(F=1) \rightarrow 5P_{1/2}(F'=2)$ transition passes through the atoms, which are imaged onto a charge-coupled device (CCD) camera. The imaging lens system is a pair of commercial achromats that give an aberration-limited resolution of approximately 5μm. Images are analyzed to deduce the number and distribution of atoms contained in the different microtraps. We make use of a calibrated absorption method for absolute number measurements [15]. When the fluence of the imaging pulse is sufficient to remove all the atoms from the $F=1$ state, the average number of photons absorbed per atom is given simply from the fluorescence branching ratios to be two. The number of atoms is then directly determined from the camera quantum efficiency and the transmission of the lenses. For small numbers of atoms and for time-of-flight temperature measurements, an additional laser tuned to repump the atoms back to $F=1$ can be used to artificially increase the number of photons absorbed per atom.

After loading atoms into the HAT at densities of 3×10^{14} cm^{-3} and temperatures of 60 μK, the atoms are distributed over typically five Talbot fringes, with each Talbot fringe typically containing 25 occupied microtraps of slightly differing trap depths. Atoms in these microtraps have sufficiently high collision rates (20 000/s) to initiate forced evaporative cooling. Using established protocols [16,17], we gently reduce the HAT intensity, allowing high kinetic energy atoms to escape while retaining low energy atoms and thereby increasing phase space density. The evaporation process tightly couples the trap depth U and the temperature so that $T \approx U/10$. During evaporation, the density n scales as the atom number N; the phase space density ρ scales as $N\nu^3/T^3 \propto n/U^{3/2}$. Even though the density and the collision rates decrease with time, they are sufficiently high in the HAT that the limit on the evaporation speed is the required adiabaticity of the z motion and the desire not to remove too many atoms. Note that the HAT has inequivalent trapping sites; sites towards the edge of the trap are more weakly bound than those at the center. Though evaporation causes the total number in all sites to decrease, atom loss in the outer sites is greater, causing the fraction of atoms contained in the central microtrap to increase from an initial 6% to nearly 15%. Atom densities and phase space densities as a function of time are shown in Fig. 2.

After evaporating to a final temperature T_e and a center microtrap density n_e, typically 1 μK and 8×10^{13} cm^{-3}, we recompress the cloud by adiabatically returning the trap depth to its maximum value U_0. Since the trap depth increases more rapidly than the temperature, this shuts off evaporation, holding the number of atoms constant in the absence of loss mechanisms. The phase space density is conserved for an adiabatic process, thus $T \propto \nu \propto U^{1/2}$ and $n \propto N\nu^3/T^{3/2}$. As a result, the recompressed density is $n_r = n_e(U_0/U_e)^{3/4}$. In our case, this gives a factor of 20 density increase, consistent with our measured final density of $1.8 \pm 0.5 \times 10^{15}$/cm^3.

A simple argument shows that the final attainable density using this method depends not only on the phase space density ρ_e achieved from evaporation, but the temperature T_e as well. The density n_e after evaporation is proportional to the product $\rho_e T_e^{3/2}$. The compression factor is $(U_0/U_e)^{3/4} \propto T_e^{-3/4}$ for fixed U_0, hence the highest density is achieved when evaporating to a U_e that maximizes the function $\rho_e T_e^{3/4}$ (see inset to Fig. 3). Continuing to lower U_e does not achieve higher densities. Evaporating to lower trap depths takes increasingly more time due to the adiabatic constraints. Losses from heating mechanisms and background collisions cause $\rho_e T_e^{3/4}$ to slowly decrease. This effectively determines the optimum value of U_e at which to start the recompression. Even with this constraint on U_e, it is interesting to point out the wide range of densities attainable with this method.

We show recompression data for various values of U_e in Fig. 3. Like evaporation, the limiting time scale for recompression is adiabaticity. Unlike evaporation, the number of atoms is conserved so the potential can be ramped up rapidly without waiting for collisional rethermalization. Figure 3 shows that even at the lowest values of U_e, densities over 10^{15} cm^{-3} can be achieved in less than 900 ms. The potential for the $U_e = 10$ μK data in Fig. 3 was raised faster than normal adiabatic constraints would advise to limit losses due to background collisions and heating mechanisms. The effect is

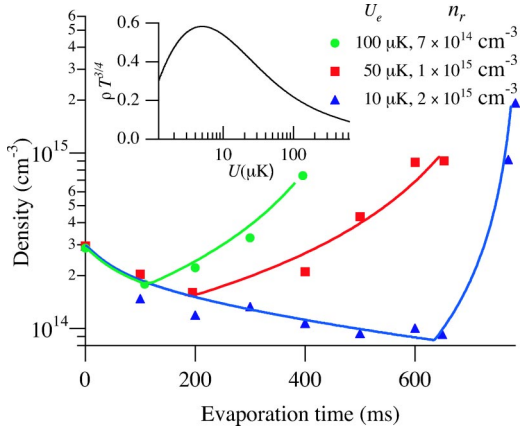

FIG. 3. Compression data and model for the center microtrap (solid line) for three values of U_e. The inset shows how the key parameter $\rho T^{3/4}$ varies with trap depth.

a small breakdown of the scaling ratios which assume perfect adiabaticity.

The high densities are deduced from measurements of the number of atoms, the fraction of atoms in each microtrap, the temperature, and direct measurements of the trap spring constants. The latter are obtained using the parametric heating method [18]. We confirm the inferred densities using measurements of known three-body recombination rates and by imaging the z axis spatial distribution. The three-body recombination rates are determined by measuring the number of atoms in the recompressed central microtrap as a function of time after recompression: $dN/dt=-K\int n(t)^3 dV-\Gamma N$, where K is the three-body recombination rate coefficient and Γ the loss rate due to background collisions. Data are shown in Fig. 4. After recompression the temperature is too small to allow evaporation. However, heating mechanisms increase the temperature with time. As a result, $n(t)$ decreases due to both recombination losses and temperature increases. Taking these effects into account, we find $K=3.5\pm1.9\times10^{-29}$ cm^6/s, in close agreement with previous measurements [19,20]. We have measured the rate in a magnetic field

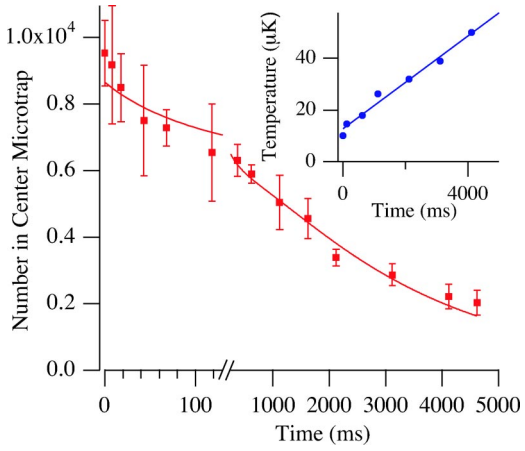

FIG. 4. After recompression we observe rapid atom loss due to three-body recombination. Since there is no evaporation from the recompressed clouds, we can measure trap heating rates by directly measuring dT/dt (inset).

of 2.5 G typically present in magnetic traps. At this field we measure $K=4.8\pm2.3\times10^{-29}$ cm^6/s. These results are extremely sensitive to density errors; the agreement with previous experiments is confirmation of the reliability of the density measurements.

We have also confirmed the densities by measuring cloud sizes. After evaporation and recompression, the semiminor axis of the cloud is only 430 nm, too small to optically resolve. However, the z axis size of 10.8 μm at 13 μK is resolvable. The measured z axis sizes agree to within 0.5 μm with the value $\sigma=\sqrt{2T/m\omega^2}$ expected from the frequency and temperature measurements, once optical resolution and motion of the atoms during the imaging pulse are taken into account. Broadening due to the superposition of multiple microtraps in our image is negligible.

In addition to using evaporation followed by recompression to produce high densities, it can be used to produce strong confinement of the atoms. During evaporation, the spatial dimensions σ of the atom clouds are unchanged since both T and ω^2 scale linearly with trap depth. During recompression $T\propto\omega$ so that $\sigma\propto(U_0/U_b)^{1/4}$ yields up to a factor of four in size reduction for trap depth ratios have observed are inferred from this ratio and the measured trap depth of 2 μK to have $\sigma=5.6$ μm. The smallest clouds for which we have a direct temperature measurement have $\sigma=8$ μm.

We now evaluate these results in the context of the Rydberg blockade. We imagine a two-photon excitation to ns Rydberg states with both lasers having a Gaussian beam of waist 10 μm. For nonuniform excitation, the appropriate figure of merit is the Rydberg-Rydberg level shift $\bar{\Omega}$ defined via $1/\bar{\Omega}^2=\langle|1/\Omega_{ij}|^2\rangle$ averaged over all atom pairs ij. Using calculated ns-ns potentials [9] with $n=(70,95)$, we find $\bar{\Omega}=(2.7,77)$ MHz for $\sigma=5.6$ μm, and $\bar{\Omega}=(1.4,40)$ MHz for $\sigma=8.0$ μm. For a collective 2-μs π pulse, the probability of double excitation even in the worst case of $\bar{\Omega}=1.4$ MHz is 1.5%. Thus these clouds are extremely well suited to investigate high-speed, high-fidelity collective coherent quantum manipulations [10].

A stronger Rydberg-Rydberg interaction can be generated by applying a static electric field and inducing a permanent dipole moment on the atoms. However, the resulting dipole-dipole interaction is zero when the interatomic axis is oriented 54.7° from the electric field direction; such pairs would experience no blockade. In the HAT, the nearly one-dimensional (1D) atom distribution mitigates this problem, and we estimate $\bar{\Omega}>135$ MHz.

For some applications, it may be useful to isolate a single microtrap from the others. To do this, we exploit the anisotropy of the microtraps to parametrically heat the atoms in the outer microtraps with little disturbance to the atoms contained in the central microtrap. The quality factor for our parametric heating experiment is about 10 for the x direction, sufficient to give significant differentiation of the 3% difference in oscillation frequencies between the center and outer microtraps. Thus we drive the parametric resonance at its low frequency tail, selectively heating and ejecting the atoms from the outer microtraps. We have been able to increase the center well fraction from 15% to above 40%.

In addition to its utility for generating high densities and

small clouds, adiabatic recompression also allows direct measurements of trap heating rates. Under conditions of evaporation, heating mechanisms do not actually increase the temperature when evaporation is rapid enough to recool the atoms by atom loss. However, evaporation no longer functions after recompression, and heating rates can be deduced directly from measured temperature increases with time. Example data are shown in the inset to Fig. 4. The deduced heating rate $dE/dt=3dT/dt$ is a factor of 1.4 larger than the predictions of Bali *et al.* [21] for quantum diffractive heating. Indeed, taking this measured heating rate into account in our evaporation model, combined with the heating due to multiple scattering as predicted by Beijerinck [22], we generate the solid curve in Fig. 2 that accounts for our measured phase space density as a function of time.

The experiments we have described represent a robust method for producing the kinds of high density ($>10^{15}$ cm^{-3}) and small size clouds (<8 μm) of interest for Rydberg atom studies both in the high-density regime of ultracold plasmas and molecular spectroscopy, and in the small-size regime relevant to coherent single-atom manipulation for quantum information processing. Many other proposed applications, including deterministic single atom and photon sources [23] and fast quantum state detection and transmission schemes [24], require these types of sources for their operation.

This work was supported by the NSF and NASA. We appreciate discussions with M. Saffman, C. Greene, B. Esry, J. Thomas, and H. Beijerinck.

[1] C. Simien *et al.*, Phys. Rev. Lett. **92**, 143001 (2004); T. Pohl, T. Pattard, and J. M. Rost, *ibid.* **92**, 155003 (2004); A. Walz-Flannigan, J. Guest, J.-H. Choi, and G. Raithel, Phys. Rev. A **69**, 063405 (2004); T. Gallagher *et al.*, J. Opt. Soc. Am. B **20**, 1091 (2003); J. L. Roberts, C. D. Fertig, M. J. Lim, and S. L. Rolston, Phys. Rev. Lett. **92**, 253003 (2004).

[2] J. Hald, J. L. Sorensen, C. Schori, and E. S. Polzik, Phys. Rev. Lett. **83**, 1319 (1999); A. Kuzmich, L. Mandel, and N. P. Bigelow, *ibid.* **85**, 1594 (2000).

[3] C. H. van der Wal *et al.*, Science **301**, 196 (2003).

[4] C. W. Chou, S. V. Polyakov, A. Kuzmich, and H. J. Kimble, Phys. Rev. Lett. **92**, 213601 (2004).

[5] C. H. Greene, A. S. Dickinson, and H. R. Sadeghpour, Phys. Rev. Lett. **85**, 2458 (2000).

[6] C. Boisseau, I. Simbotin, and R. Cote, Phys. Rev. Lett. **88**, 133004 (2002).

[7] S. Farooqi *et al.*, Phys. Rev. Lett. **91**, 183002 (2003).

[8] M. D. Lukin *et al.*, Phys. Rev. Lett. **87**, 037901 (2001).

[9] T. G. Walker and M. Saffman, e-print physics/0407048 (2004).

[10] D. Tong *et al.*, Phys. Rev. Lett. **93**, 063001 (2004).

[11] K. Singer *et al.*, Phys. Rev. Lett. **93**, 163001 (2004).

[12] An additional requirement is that the Rydberg-Rydberg interaction has no dipole-dipole zeros. See Ref. [9].

[13] R. Newell, J. Sebby, and T. Walker, Opt. Lett. **28**, 1266 (2003).

[14] M. H. Anderson, W. Petrich, J. R. Ensher, and E. A. Cornell, Phys. Rev. A **50**, R3597 (1994).

[15] K. E. Gibble, S. Kasapi, and S. Chu, Opt. Lett. **17**, 526 (1992).

[16] K. Davis, M.-O. Mewes, and W. Ketterle, Appl. Phys. B: Lasers Opt. **60**, 155 (1995).

[17] K. M. O'Hara, M. E. Gehm, S. R. Granade, and J. E. Thomas, Phys. Rev. A **64**, 051403 (2001).

[18] S. Friebel *et al.*, Appl. Phys. B: Lasers Opt. **B67**, 699 (1998).

[19] E. A. Burt *et al.*, Phys. Rev. Lett. **79**, 337 (1997).

[20] B. L. Tolra *et al.*, Phys. Rev. Lett. **92**, 190401 (2004).

[21] S. Bali *et al.*, Phys. Rev. A **60**, R29 (1999).

[22] H. C. W. Beijerinck, Phys. Rev. A **62**, 063614 (2000).

[23] M. Saffman and T. G. Walker, Phys. Rev. A **66**, 065403 (2002).

[24] M. Saffman and T. G. Walker, e-print quant-ph/0402111 (2004).